FASEB journal (2018.5) 32(5):2354-2365.

Prostaglandin I2 suppresses the development of diet-induced nonalcoholic steatohepatitis in mice.

Shima Kumei, Koh-Ichi Yuhki, Fumiaki Kojima, Hitoshi Kashiwagi, Yoshitaka Imamichi, Toshikatsu Okumura, Shuh Narumiya, Fumitaka Ushikubi

Prostaglandin I_2 suppresses the development of diet-induced nonalcoholic steatohepatitis in mice

Running title: The role of PGI_2 in NASH

Shima Kumei, research associate, Department of Pharmacology and General Medicine, Asahikawa Medical University, Asahikawa, Japan

Midorigaoka higashi 2-1-1-1, Asahikawa, Hokkaido, 078-8510, Japan

kumei@asahikawa-med.ac.jp

Koh-ichi Yuhki, associate professor, Department of Pharmacology, Asahikawa Medical University, Asahikawa, Japan

Midorigaoka higashi 2-1-1-1, Asahikawa, Hokkaido, 078-8510, Japan

yukik@asahikawa-med.ac.jp

Fumiaki Kojima, assistant professor, Department of Pharmacology, Asahikawa Medical University, Asahikawa, Japan

Midorigaoka higashi 2-1-1-1, Asahikawa, Hokkaido, 078-8510, Japan

kojimaf@kitasato-u.ac.jp

Hitoshi Kashiwagi, assistant professor, Department of Pharmacology, Asahikawa Medical University, Asahikawa, Japan

Midorigaoka higashi 2-1-1-1, Asahikawa, Hokkaido, 078-8510, Japan

h-kashi@asahikawa-med.ac.jp

Yoshitaka Imamichi, assistant professor, Department of Pharmacology, Asahikawa Medical University, Asahikawa, Japan

Midorigaoka higashi 2-1-1-1, Asahikawa, Hokkaido, 078-8510, Japan

imamichi@asahikawa-med.ac.jp

Toshikatsu Okumura, professor, Department of General Medicine, Asahikawa Medical University, Asahikawa, Japan

Midorigaoka higashi 2-1-1-1, Asahikawa, Hokkaido, 078-8510, Japan

okumurat@asahikawa-med.ac.jp

Shuh Narumiya, professor, Department of Pharmacology, Kyoto University Faculty of Medicine, Kyoto, Japan

Yoshida-Konoe-cho, Sakyo-ku, Kyoto, 606-8315, Japan

snaru@mfour.med.kyoto-u.ac.jp

Fumitaka Ushikubi, professor, Department of Pharmacology, Asahikawa Medical

University, Asahikawa, Japan

Midorigaoka higashi 2-1-1-1, Asahikawa, Hokkaido, 078-8510, Japan

ushikubi@asahikawa-med.ac.jp

Correspondence:

Fumitaka Ushikubi

Midorigaoka higashi 2-1-1-1, Asahikawa, Hokkaido, Japan

ushikubi@asahikawa-med.ac.jp

Tel: 81-166-68-2360 Fax: 81-166-68-2369

Conflicts of interest: The authors disclose no conflicts.

Author Contributions:

Designing research studies: S.K., T.O., S.N., and F.U.

Conducting experiments: S.K., K.Y., F.K., H.K., and Y.I.

Analyzing data: S.K., and K.Y.

Writing the manuscript: S.K., K.Y., T.O., and F.U.

Nonalcoholic steatohepatitis (NASH) is a hepatic manifestation of metabolic syndrome. Although the prostaglandin (PG) I_2 receptor IP is expressed broadly in the liver, the role of PGI_2-IP signaling in the development of NASH remains to be determined. Here, we investigated the role of the PGI_2-IP system in the development of steatohepatitis using mice lacking the PGI_2 receptor IP (IP-KO mice) and a specific IP agonist beraprost. IP-KO and wild-type (WT) mice were fed a methionine- and choline-deficient diet (MCDD) for 2, 5, or 10 wk. Beraprost was administrated orally to mice every day during the experimental periods. The effect of beraprost on the expression of chemokine and inflammatory cytokines was examined also in cultured Kupffer cells. WT mice fed MCDD developed steatohepatitis at 10 wk. Interestingly, IP-KO mice had earlier development of steatohepatitis at 5 wk with augmented histological derangements, accompanied by increased hepatic monocyte chemoattractant protein-1 (MCP-1) and tumor necrosis factor (TNF)-α contents. After 10 wk of MCDD, IP-KO mice had greater hepatic iron deposition with prominent oxidative stress, resulting in hepatocyte damage. In WT mice, beraprost improved histological and biochemical parameters of steatohepatitis, accompanied by reduced hepatic contents of MCP-1 and TNF-α. Accordingly, beraprost suppressed the lipopolysaccharide stimulated *Mcp-1* and *Tnf-α* mRNA expression in cultured Kupffer cells prepared from WT mice. PGI_2-IP signaling plays a crucial role in the development and progression of steatohepatitis by modulating the inflammatory response leading to augmented oxidative stress. We suggest that the PGI_2-IP system is an attractive therapeutic target for NASH treatment.

Keywords: prostaglandin; Kupffer cell; NASH; oxidative stress

Nonalcoholic fatty liver disease (NAFLD) is a manifestation of metabolic syndrome in the liver (1-3). NAFLD can be divided into two categories, benign simple steatosis and nonalcoholic steatohepatitis (NASH). NASH is associated with increased risks for cirrhosis and hepatocellular carcinoma. With growing number of NASH patients, NASH has become a global public health issue. Although the pathogenic mechanism of NASH has remained poorly understood, the most widely accepted idea explaining the pathogenesis of NASH is the "two hits" hypothesis (4). The first hit is fatty liver, which is frequently associated with obesity, type 2 diabetes mellitus and hyperlipidemia. Major candidates for the second hit are augmented oxidative stress and cytokine production (5). The "multiple parallel hits" hypothesis, a hypothesis that steatohepatitis develops in parallel to steatosis, has also been proposed based on recent studies (6). However, the precise pathogenic mechanisms by which steatosis is transformed to steatohepatitis remain to be clarified, and there are few established therapeutic strategies for NASH (5, 7).

Cyclooxygenase (COX)-2, the inducible isozyme for prostanoid biosynthesis, is expressed highly in the liver of NASH patients (8). Up-regulation of hepatic COX-2 expression was also observed in murine NASH models (9-11). In methionine- and choline-deficient diet (MCDD)-induced NASH, hepatic expression level of COX-2 was 10-fold higher than that in control mice, and selective COX-2 inhibitors ameliorated the severity of steatohepatitis, suggesting a proinflammatory role of COX-2 in the NASH pathogenesis (9). However, little attention has been paid to the association between each prostanoid and NASH, and which type(s) of prostanoids participates in the pathogenesis of

NASH remains to be clarified.

Prostaglandin (PG) I_2 is synthesized by PGI synthase (PGIS) following COX-catalyzed generation of PGH_2, and it plays various roles in the body via its specific receptor IP (12). Historically, PGI_2 has been known to play a role in maintenance of the cardiovascular system, in which PGI_2 works as a potent vasodilator and as an anti-platelet agent (13, 14). Accordingly, IP agonists have been widely used as therapeutic agents for pulmonary arterial hypertension (15) and preventive agents against thrombotic diseases. In addition, novel roles of PGI_2 in the cardiovascular system have been clarified; PGI_2 protects the heart from ischemia-reperfusion injury (16), suppresses the development of cardiac hypertrophy (17), and works as a mediator of renin secretion in renovascular hypertension (18). In the liver, PGI_2 modulates sinusoidal microcirculation by regulating contraction of hepatic stellate cells (HSCs) (19). However, IP is expressed broadly on the cells constituting the liver including hepatocytes, sinusoidal endothelial cells, Kupffer cells and HSCs (20-22), all of which are also able to produce PGI_2 (23-27). In addition, increasing attention has been paid to the anti-inflammatory roles of PGI_2 in the development of inflammatory diseases of several organs including the liver (28). Beraprost, an IP agonist, decreased liver tissue damage in a mouse model of concanavalin-A-induced hepatitis (29), and iloprost, another IP agonist, protected mice from galactosamine-lipopolysaccharide (LPS)-induced fulminant hepatitis (30). However, the role of the PGI_2-IP system in the development of NASH remains to be elucidated.

MCDD is widely used to induce the development of steatohepatitis in a rodent model

of NASH. Since choline is essential for hepatic secretion of very low-density lipoprotein (31), its deficiency impairs hepatic lipoprotein secretion and induces hepatic steatosis. Choline deficiency also changes the composition of the mitochondrial membrane, resulting in mitochondrial dysfunction and facilitating the development of steatohepatitis. In addition, choline and methionine are required for the production of S-adenosylmethionine, a universal donor of methyl groups that protects the liver from oxidative stress induced by elevation of hepatic glutathione levels. Accordingly, S-adenosylmethionine prevents hepatic damage in alcoholic liver disease and CCl_4-induced hepatitis (32). These mechanisms participate to induce the development and progression of steatohepatitis in mice fed MCDD. In this study, we attempted to clarify the role of the PGI_2-IP system in the development of NASH using an MCDD-induced NASH model and mice lacking IP (IP-KO mice).

Materials and Methods

Animals

The generation of IP-KO mice was reported (33). IP-KO and WT control mice have the genetic background of C57BL/6 mice. All experiments were performed using 8- to 10-week-old male mice, which were maintained under a controlled condition (22°C room temperature, 50-60% humidity, 12-hour light/dark cycles). All of the animal studies were approved by the Asahikawa Medical University Committee on Animal Research.

Diet-induced NASH model

Mice were fed MCDD (Oriental Yeast Company, Tokyo, Japan) or normal diet (ND; Oriental Yeast Company). At the end of the experiments, blood glucose level was determined using a glucose meter (Medisafe Mini GR-102; TERUMO, Tokyo, Japan). Then mice were anesthetized with diethyl ether, and blood was collected by cardiac puncture for biochemical analyses in the non-fasted state. The liver was excised and fixed in 4% phosphate-buffered paraformaldehyde for histological and immunohistochemical examinations. A part of the liver was snap-frozen in liquid nitrogen and stored at -80°C for later analyses of triglycerides (TG), thiobarbituric acid-reactive species (TBARS), and cytokines, monocyte chemoattractant protein-1 (MCP-1) and tumor necrosis factor (TNF)-α.

When examining the *in vivo* effect of beraprost (Toray Industries, Inc., Tokyo, Japan) (34), it was dissolved in saline and administered to mice by oral gavage once a day at a

dose of 1.0 mg/kg.

Histological and immunohistochemical examinations

NAFLD activity score was used for evaluation of histological change of the liver induced by MCDD feeding (35), which score was determined using hematoxylin and eosin (HE)-stained sections (4 μm in thickness) by two blinded investigators. Briefly, steatosis ranged from 0 to 3 (0: <5%, 1: 5–33%, 2: 33–66%, 3: >66% of parenchymal involvement), inflammatory foci ranged from 0 to 3 (0: none, 1: <2, 2: 2–4, 3: >4 foci per 200 x field), and hepatocyte degeneration ranged from 0 to 2 (0: none, 1: 1 or 2, 2: >2 cells showing ballooning degeneration per 200 x field). NAFLD activity score represents the sum of these three scores. We assumed that steatohepatitis comparable to NASH has developed when the NAFLD activity score exceeds 5 according to a previous human study on NASH (35). To assess fat accumulation, frozen liver sections were stained with Oil Red O (Muto Pure Chemicals, Tokyo, Japan). Tissue sections were also stained with Berlin-blue to evaluate hepatic iron accumulation.

For immunohistochemical examinations of inflammatory cell infiltration and oxidative stress, deparaffinized sections were incubated with their respective primary antibodies: anti-F4/80 antibody (T-2008; BMA Biochemicals AG, Augst, Switzerland) (36) and anti-4-hydroxy-2-nonenal (4-HNE) antibody (ab46545; Abcam, Cambridge, UK) (37), followed by incubation with peroxidase-conjugated secondary antibodies: anti-rat IgG antibody (Histofine Simple Stain RAT MAX PO, Nichirei, Tokyo, Japan) for anti-F4/80

antibody and anti-rabbit IgG antibody (Histofine Simple Stain RABBIT, MAX PO Nichirei) for anti-4-HNE antibody. The positive signals were visualized with DAB (Histofine Simple Stain DAB, Nichirei).

Biochemical analyses

Serum concentrations of AST, ALT, TG, total cholesterol (T-chol) and ferritin were measured by an automatic analyzer (7180; Hitachi High-Technologies Corporation, Tokyo, Japan). For measurement of hepatic iron contents, lyophilized liver tissues were treated with nitric acid and perchloric acid, and iron contents were determined by atomic absorption spectrophotometry (Z-8200; Hitachi High-Technologies Corporation) (38). For measurement of hepatic lipid contents, a piece of the liver (100 mg) was homogenized in 1.5 mL of $CHCl_3$/MeOH (2:1). After sequential centrifugation procedures, the organic phase containing the lipid was separated and stored at -80°C until use. At the time of measurement, the sample (200 μL) was mixed with 40 μL of TritonX-100/$CHCl_3$ (1:1), and $CHCl_3$ was evaporated. The resulting Triton film was dissolved in 200 μL of distilled water, and the lipid concentration was determined using an automatic analyzer (7180; Hitachi High-Technologies Corporation). Lipid peroxidation in the liver was examined by measuring TBARS using a TBARS Assay Kit (Cayman Chemical, Ann Arbor, MI).

Real-Time PCR

Real-time PCR was performed as described (39). In short, isolated total RNA was

reverse-transcribed using SuperScript VILO (Invitrogen, Carlsbad, CA). Real-time PCR was performed using TaqMan primers and probes (Applied Biosystems, Foster City, CA) for *Cox-1* (Mm 00477214), *Cox-2* (Mm 00478374), *Ip* (Mm 00801939), *Pgis* (Mm 00447271), *18s* rRNA (Mm 03928990), *Mcp-1* (Mm00441242), and *Tnf-α* (Mm 00443258).

ELISA

The hepatic contents of MCP-1 and TNF-α were determined using ELISA kits for mouse MCP-1 and TNF-α, respectively (Quantikine ELISA kits; R & D Systems, Minneapolis, MN). To evaluate PGI_2 production by cultured Kupffer cells and hepatocytes, the contents of 6-keto $PGF_1\alpha$, a stable metabolite of PGI_2, in the conditioned medium was measured using an EIA kit (Cayman Chemical).

Assays using primary cultured Kupffer cells and hepatocytes

The liver was perfused through a canula inserted into the inferior vena cava with Ca^{2+}- and Mg^{2+}-free HBSS (CMF-HBSS), followed by perfusion with HBSS containing collagenase II (0.1%) for 30 min at 37°C. Then the liver was dispersed, and the cell suspension was filtered through a nylon mesh (pore size of 100 μm). After hepatocytes had been sedimented and collected by centrifugation at 40 x g for 1 min at 4°C, the supernatant containing nonparenchymal cells was further centrifuged at 550 x g for 4 min. The pellet of nonparenchymal cells was suspended in CMF-HBSS containing bovine serum albumin (0.1%), and Kupffer cells were separated by centrifugation using density gradient

medium (OptiPrep; Axis-Shield, Oslo, Norway). For examination of mRNA expression of cytokines, MCP-1 and TNF-α, the cells (2.0×10^6) were seeded in RPMI1640 containing 10% FBS, 100 U/mL penicillin, and 100 μg/mL streptomycin using 35 mm culture dish. After 15 min of the seeding procedure, attached Kupffer cells were further cultured in RPMI1640 containing 10% FBS for 15 h. After 4 h of serum starvation, the medium was replaced by RPMI1640 containing indomethacin (10 μmol/L), and the cells were stimulated with LPS (25 ng/mL) for 5 h. Beraprost was added 30 min before the addition of LPS. Total RNA of cultured Kupffer cells or hepatocytes was extracted with a QIAGEN QIAshredder and RNeasy MINI kit (QIAGEN, Hilden, Germany).

For measurement of PGI_2 production, Kupffer cells (5×10^5) were seeded in RPMI1640 containing 10% FBS using a 24-well culture plate. After 24 h of culture, Kupffer cells were washed two times with serum-free RPMI1640 containing 0.1% bovine serum albumin. After 4 h of serum starvation, the cells were stimulated with LPS (25 ng/mL) for 24 h. Hepatocytes (4.5×10^5) were seeded in Williams' E medium containing 10% FBS, 100 U/mL penicillin, and 100 μg/mL streptomycin using a 35 mm primaria culture dish (Corning Co., Corning, NY). After 4 h of the seeding procedure, unattached cells were removed by washing, and attached hepatocytes were further cultured in Williams' E medium containing 10% FBS for 24 h. After 24 h of culture, hepatocytes were washed two times with serum-free Williams' E medium containing 0.1% bovine serum albumin and stimulated with LPS (25 ng/mL) for 24 h. Then the conditioned medium was collected, frozen, and stored at -80°C until use.

RT-PCR

Total RNA of cultured Kupffer cells was extracted with QIAGEN QIAshredder and RNeasy MINI kit (QIAGEN). One μg RNA was reverse-transcribed using SuperScript VILO (Invitrogen). The *Ip* mRNA expression in Kupffer cells was determined by PCR using Gene Taq (Nippon Gene, Toyama, Japan) as reported (17).

Statistical Analysis

All values are expressed as means ± SEM. For comparison of two groups, Student's or Welch's t-test was performed after carrying out the *F*-test for equal variance. Comparison of more than two groups was performed with one-way or two-way ANOVA followed by Dunnett's multiple comparison test or Sidak's post test, respectively. A *P* value < .05 was considered statistically significant.

Results

MCDD induces up-regulation of hepatic expression of Cox-2, Pgis and Ip mRNAs in WT mice

The expression level of *Cox-2* mRNA was increased significantly after 10 wk of MCDD, while the expression level of mRNA for *Cox-1*, the constitutively expressed isoform of COXs, did not change significantly (Figure 1A). The expression level of *Pgis* mRNA was also increased significantly after 10 wk of MCDD (Figure 1B). The expression level of *Ip* mRNA was increased after 2 wk of MCDD and reached a significantly high level after 10 wk of MCDD (Figure 1C). These results indicate that PGI_2-IP signaling is reinforced during MCDD feeding and that the PGI_2-IP system might participate in the development of NASH.

Development of steatohepatitis induced by MCDD is facilitated in IP-KO mice

To determine whether the PGI_2-IP system participates in the development of steatohepatitis, we fed WT and IP-KO mice with MCDD and examined histological change of the liver. After 5 wk of MCDD, the livers of WT mice showed mild steatosis (Figure 2A) with an NAFLD activity score of 3.4 ± 0.6 (Figure 2B). The livers of WT mice fed MCDD for 10 wk, however, showed histological characteristics of steatohepatitis including increased steatosis, inflammatory cell infiltration and hepatocyte degeneration (Figure 2A and C) with an NAFLD activity score of 6.3 ± 0.3 (Figure 2B), indicating the development of steatohepatitis that is comparable with human NASH (35). It is noteworthy that the

livers of IP-KO mice showed augmented histological derangements after 5 wk of MCDD (Figure 2A) with an NAFLD activity score of 5.8 ± 0.4 (Figure 2B), indicating an early onset of steatohepatitis in IP-KO mice. The scores for all three parameters were significantly higher in IP-KO mice fed MCDD for 5 wk than those in WT mice (Figure 2C). However, there was no significant difference in the NAFLD activity score after 10 wk of MCDD between IP-KO and WT mice, because the scores had almost reached the maximum scores after 10 wk of MCDD in both genotypes, while apparent histological change of the liver was much more drastic in IP-KO mice than in WT mice (Figure 2A). In addition to the induction of steatohepatitis, MCDD feeding induced changes in nutritional and metabolic conditions as reported previously (40). There were no significant differences between these parameters in IP-KO and WT mice except for a slight difference in body weight at the start of MCDD feeding (Table 1).

To further assess the degree of steatosis, Oil Red O staining was performed after 5 wk of MCDD. IP-KO mice showed striking fat deposition in hepatocytes compared with that in WT mice (Figure 3A). Quantification of TG from liver lysates also demonstrated a significant increase in TG contents in the livers of IP-KO mice than those in the livers of WT mice (Figure 3B). Since Kupffer cells and blood-derived macrophages are thought to play a central role in this model (41), we investigated the degree of infiltration of these cells by counting F4/80-positive cells after 5 wk of MCDD. As expected, the number of F4/80-positive cells (brown color) in the IP-KO liver was significantly higher than that in the WT liver (Figure 3C and D). In addition to histopathological assessment, we

measured serum transaminase levels for the evaluation of hepatocyte damage. The levels of serum AST and ALT in IP-KO mice were significantly higher than those in WT mice after 5 wk of MCDD (Figure 3E). These histological and biochemical findings clearly indicate that the progression of steatohepatitis is accelerated in IP-KO mice during 5 wk of MCDD.

Augmented iron deposition and oxidative stress in the liver of IP-KO mice

We next measured hepatic iron contents by atomic absorption spectrophotometry to determine whether hepatic iron was associated with progression of MCDD-induced steatohepatitis in IP-KO mice. Hepatic iron contents increased gradually during feeding with MCDD in both WT and IP-KO mice (Figure 4A). Interestingly, hepatic iron contents were significantly higher in IP-KO mice than in WT mice after 10 wk of MCDD (Figure 4A), suggesting the involvement of hepatic iron in the progression of steatohepatitis. In accordance with the levels of hepatic iron contents, serum ferritin levels increased gradually during feeding with MCDD in both WT and IP-KO mice, and the level was significantly higher in IP-KO mice than in WT mice after 10 wk of MCDD (Figure 4B). To determine the localization of iron deposition in the liver, hepatic iron was stained with Berlin blue after 10 wk of MCDD. Reflecting the levels of hepatic iron contents, the blue staining was clearly stronger in the livers of IP-KO mice than in the livers of WT mice, and the signal was localized mainly in the cytoplasm of hepatocytes (Figure 4C and D). Although iron was localized mainly in hepatocytes, immunohistochemical staining with

anti-F4/80 antibody showed iron accumulation also in some F4/80-positive cells (Figure 4D).

To explore the mechanism of the increased progression of steatohepatitis in IP-KO mice, we examined whether hepatic iron overload results in increased oxidative stress. We performed immunohistochemical staining of 4-HNE, a representative lipid peroxide product, in the liver. The 4-HNE staining (brown color) was much stronger in the livers of IP-KO mice than in the livers of WT mice after 10 wk of MCDD (Figure 4E). In addition, the hepatic level of TBARS, a marker of lipid peroxidation, was significantly higher in IP-KO mice than in WT mice after 10 wk of MCDD (Figure 4F), suggesting that hepatic iron overload led to augmented oxidative stress in IP-KO mice. These results indicate that increased oxidative stress contributes to the progression of steatohepatitis in IP-KO mice, especially at a later phase (10 wk of MCDD feeding).

Increased production of MCP-1 and TNF-α in the liver of IP-KO mice fed MCDD

We next examined whether chemokines and cytokines, which are considered to be the second hits for the development of steatohepatitis, participate in the progression of steatohepatitis in IP-KO mice. In WT mice, the hepatic contents of monocyte chemoattractant protein-1 (MCP-1), a representative chemokine for the recruitment of macrophages, were increased after 2 wk of MCDD and reached a significantly higher level after 5 wk of MCDD (Figure 4G). In IP-KO mice, the hepatic contents of MCP-1 increased gradually and reached a significantly higher level after 10 wk of MCDD, which

level was significantly higher than that in WT mice (Figure 4G). In WT mice, the hepatic contents of TNF-α, a representative cytokine responsible for the development of NASH (42), were increased significantly after 2 wk of MCDD and remained at similar levels thereafter (Figure 4H). In IP-KO mice, the hepatic contents of TNF-α were increased significantly after 5 wk of MCDD, and the level was significantly higher than that in WT mice (Figure 4H). These results suggest that increased MCP-1 and TNF-α production in the liver participates in the progression of steatohepatitis in IP-KO mice.

Suppressive effects of beraprost, an IP agonist, on the progression of MCDD-induced steatohepatitis

Because a lack of IP signaling facilitated the progression of MCDD-induced steatohepatitis, we next examined whether stimulation of IP by beraprost would attenuate the progression of steatohepatitis. In WT mice, beraprost significantly suppressed the progression of steatohepatitis after 10 wk of MCDD: NAFLD activity scores in the control and beraprost-treated groups were 6.3 ± 0.3 and 3.8 ± 0.6, respectively (Figure 5A and B). In IP-KO mice, beraprost failed to suppress the progression of steatohepatitis (Figure 5A), and there was no significant improvement in the NAFLD activity score (Figure 5B). The suppressive effect of beraprost on inflammatory cell infiltration was remarkable, but there was no significant effect on steatosis (Figure 5C). Accordingly, beraprost significantly suppressed F4/80-positive cell accumulation in the livers of WT mice after 10 wk of MCDD (Figure 5D and E). In addition, beraprost drastically suppressed the elevation of

serum AST and ALT levels in WT mice after 10 wk of MCDD, indicating that beraprost effectively reduced hepatocyte damage (Figure 5F). In IP-KO mice, beraprost again had no effect on serum AST and ALT levels (Figure 5F), indicating an IP-dependent effect of beraprost.

We further examined whether stimulation of the PGI_2-IP system would reduce the hepatic production of MCP-1 and TNF-α, the production of which was significantly augmented in IP-KO mice. Beraprost significantly reduced the hepatic content of MCP-1 in WT mice after 5 and 10 wk of MCDD (Figure 5G). Beraprost also significantly reduced the hepatic content of TNF-α in WT mice throughout the experimental periods (Figure 5H). These results suggest that beraprost suppressed the development of steatohepatitis at least by inhibiting the hepatic production of chemokine(s) and cytokine(s).

LPS stimulates PGI_2 production, and beraprost suppresses the LPS-induced expression of mRNAs for Mcp-1 and Tnf-α in cultured Kupffer cells

Since the main cell types producing MCP-1 and TNF-α in the liver are thought to be Kupffer cells and blood-derived monocytes (41), we finally examined PGI_2 production in primary cultured hepatocytes and Kupffer cells and the effect of beraprost on the expression of *Mcp-1* and *Tnf-α* mRNAs in cultured Kupffer cells. We first confirmed *Ip* mRNA expression in primary cultured Kupffer cells prepared from WT mice (Figure 6A).

Since the level of LPS, a toll-like receptor 4 agonist, within the portal vein increases in the MCDD-induced NASH model, leading to stimulation of hepatic cells and induction

of hepatic cytokine production (43), we stimulated the cultured cells with LPS. To clarify which type(s) of hepatic cells produces PGI_2, we measured the contents of 6-keto $PGF_1\alpha$, a stable PGI_2 metabolite, in the cultured media of hepatocytes and Kupffer cells after stimulation with LPS (Figure 6B). Without the stimulation, the concentration of 6-keto $PGF_1\alpha$ in the medium of hepatocytes was not measurable, while that in the medium of Kupffer cells was barely measurable and was 116 pg/mL. However, LPS drastically elevated the content of 6-keto $PGF_1\alpha$ in the conditioned medium of Kupffer cells (11,113 pg/mL), while LPS induced only a small increase in the content of 6-keto $PGF_1\alpha$ in the conditioned medium of hepatocytes (81 pg/mL). Although it is difficult to determine the precise cell type(s) producing PGI_2 in the NASH model, these results suggest that Kupffer cells at least can produce abundant PGI_2 after stimulation.

LPS remarkably up-regulated the expression levels of mRNAs for both *Mcp-1* and *Tnf-α* in cultured Kupffer cells isolated from the liver of WT mice (Figure 6C and E). Beraprost significantly suppressed the LPS-induced up-regulation of mRNAs for both *Mcp-1* and *Tnf-α*, whereas beraprost alone had no effect on the expression levels of these mRNAs (Figure 6C and E). In addition, these suppressive effects of beraprost disappeared in Kupffer cells prepared from IP-KO mice (Figure 6D and F), indicating IP-dependent effects of beraprost. These results further suggest that the PGI_2-IP system suppresses the development of steatohepatitis by inhibiting the production of MCP-1 and TNF-α by Kupffer cells.

Discussion

In the present study, we attempted to clarify the role of the PGI_2-IP system in the development of steatohepatitis. The hepatic expression levels of *Cox-2*, *Pgis* and *Ip* increased significantly in WT mice fed MCDD, indicating reinforcement of the PGI_2-IP system during MCDD feeding. IP-KO mice had earlier development of steatohepatitis after 5 wk of MCDD with increased hepatic production of MCP-1 and TNF-α. After 10 wk of MCDD, IP-KO mice had greater hepatic iron deposition with resultant prominent oxidative stress, indicating further progression of steatohepatitis in IP-KO mice. In contrast, beraprost significantly improved histological and biochemical parameters of steatohepatitis in WT mice but not in IP-KO mice. In addition, beraprost significantly reduced the hepatic production of MCP-1 and TNF-α in WT mice. Accordingly, beraprost suppressed the LPS-stimulated *Mcp-1* and *Tnf-α* mRNA expression in primary cultured Kupffer cells prepared from WT mice. These results clearly indicate that PGI_2-IP signaling plays a crucial role in the development and progression of steatohepatitis by modulating the inflammatory response that leads to augmented oxidative stress.

We showed that hepatic *Cox-2* mRNA expression is up-regulated during MCDD feeding (Figure 1A). This result suggests that COX-2-derived prostanoids are involved in the pathogenesis of NASH. In addition to *Cox-2* mRNA, the expression levels of *Pgis* and *Ip* mRNAs increased significantly during MCDD feeding (Figure 1B and C). Although the hepatic expression levels of mRNAs for the Ep_2 and Ep_4 subtype receptors of PGE_2, an inflammatory mediator, also increased by 2.0 ± 0.2 and 2.6 ± 0.3 times, respectively (data

not shown), the hepatic expression level of *Ip* mRNA was further increased by 3.7 ± 0.8 times after 5 wk of MCDD. These results suggest that PGI_2-IP signaling is reinforced during MCDD feeding and that the PGI_2-IP system plays a role in the development of steatohepatitis.

Histological analysis using NAFLD activity score after 5 wk of MCDD revealed that IP-KO mice had more severe liver inflammation comparable to steatohepatitis than that in WT mice (Figure 2). In addition, TG contents and F4/80-positive cell numbers in the liver, as well as serum transaminase levels, were significantly higher in IP-KO mice than in WT mice after 5 wk of MCDD (Figure 3). These results clearly indicate that a lack of IP signaling led to the facilitated development of steatohepatitis and suggest that endogenous PGI_2 plays a suppressive role in the progression of steatohepatitis via IP. In contrast, when IP was activated pharmacologically by beraprost, the NAFLD activity score comparable to steatohepatitis found in control mice decreased drastically (Figure 5B). In addition, beraprost remarkably suppressed the increase in serum transaminase levels in an IP-dependent manner (Figure 5F). Thus, the present study using IP-KO mice and an IP agonist has proved for the first time that the PGI_2-IP system plays a suppressive role in the development of steatohepatitis.

Infiltration of inflammatory cells into the liver plays a critical role in the initiation and progression of NASH (41). In fact, depletion of Kupffer cells reduced the degree of liver injury, steatosis, and monocyte infiltration in a murine NASH model (41). In this study, inflammatory cell infiltration started after only 2 wk of MCDD in both WT and

IP-KO mice (Figure 2C). Notably, the degree of inflammatory cell infiltration was significantly greater in IP-KO mice than in WT mice after 5 wk of MCDD (Figures 2C and 3D). In contrast, beraprost significantly suppressed inflammatory cell infiltration into the liver after 2 and 10 wk of MCDD (Figure 5C–E). These results suggest that the suppressive effect of PGI_2-IP signaling on the development and progression of steatohepatitis depends at least on the inhibition of inflammatory cell infiltration. Among chemokines, MCP-1 promotes macrophage accumulation in the liver and plays an important role in the development of NASH (44). Accordingly, MCP-1 is up-regulated in the liver of NASH patients (45), and mice lacking the MCP-1 receptor C-C chemokine receptor type 2 had reduced hepatic recruitment of macrophages in experimental steatohepatitis (46). Being consistent with inflammatory cell infiltration, hepatic contents of MCP-1 were increased after 5 wk of MCDD in both WT and IP-KO mice, and the hepatic MCP-1 level was significantly higher in IP-KO mice than in WT mice after 10 wk of MCDD (Figure 4G). In addition, beraprost significantly suppressed the increases in hepatic MCP-1 contents after 5 and 10 wk of MCDD (Figure 5G). These results indicate that the PGI_2-IP system suppresses inflammatory cell infiltration into the liver by inhibiting MCP-1 production.

The cytokine milieu in the liver also plays a critical role in the development and progression of NASH, in which the proinflammatory cytokine TNF-α, as well as interleukin-6, is a major player (6). In an MCDD-induced NASH model, the development of steatohepatitis was suppressed in mice lacking both TNF-α receptors 1 and 2 (42), and

targeted knockdown of TNF-α expression in myeloid cells suppressed the development of NASH (41). In this study, the hepatic contents of TNF-α were significantly higher after 5 wk of MCDD in IP-KO mice than in WT mice (Figure 4H), and beraprost significantly decreased the hepatic contents of TNF-α in WT mice (Figure 5H), suggesting that the PGI_2-IP system suppresses the development and progression of steatohepatitis by decreasing the hepatic TNF-α contents.

Kupffer cells are considered to be the major cell type to produce TNF-α in the liver (41), and they are both important sources of and responders to MCP-1 (44). We therefore hypothesized that PGI_2 acts on IP expressed on Kupffer cells, exerting an anti-inflammatory effect by inhibiting the production of both MCP-1 and TNF-α. To test this hypothesis, we first examined which type(s) of hepatic cells, Kupffer cells or hepatocytes, produces PGI_2, (Figure 6B) and we confirmed that Kupffer cells could produce abundant PGI_2 after LPS stimulation. We next examined the effect of beraprost on LPS-stimulated expression of mRNAs for *Mcp-1* and *Tnf-α* in primary cultured Kupffer cells prepared from WT mice. LPS was used as a stimulant for TLR4 to reproduce the condition found in the MCDD-induced NASH model, in which the levels of TLR4 agonists in the portal vein were increased (47). Since little is known about whether murine Kupffer cells express IP, we first confirmed the expression of *Ip* in these cells (Figure 6A). LPS drastically increased the expression levels of both *Mcp-1* and *Tnf-α* mRNAs in Kupffer cells, and beraprost significantly inhibited these increases in an IP-dependent manner (Figure 6C-F), indicating that PGI_2 is able to act directly on Kupffer cells and inhibit production of the

proinflammatory molecules MCP-1 and TNF-α. Although an IP agonist suppressed LPS-induced TNF-α expression in human monocytes (48), we clearly showed that Kupffer cells indeed express *Ip* and that beraprost inhibits LPS-induced expression of not only *Tnf-α* but also *Mcp-1* in Kupffer cells. These results support our hypothesis that the PGI_2-IP system suppresses the production of TNF-α both by reducing inflammatory cell recruitment into the liver and by direct inhibitory action on Kupffer cells, indicating at least partly the mechanism by which the PGI_2-IP system suppresses the development and progression of steatohepatitis. Since TNF-α plays an important role not only in inflammatory response but also in hepatic steatosis (6, 41), the increased TNF-α production may also contribute to the enhanced hepatic steatosis found in IP-KO mice.

Hepatic iron deposition is one of the factors that promote the progression of NASH through the induction of oxidative stress responses (49, 50). Hepatic iron deposition is associated with histological severity of liver disease in NASH patients (51, 52), and phlebotomy induces clinical improvement in NASH patients (53). Accordingly, serum ferritin levels were significantly higher in NASH patients than in patients with simple steatosis (54). In this study, IP-KO mice had higher hepatic iron contents (Figure 4A and C) and serum ferritin levels (Figure 4B) than those in WT mice, suggesting that excess hepatic iron accumulation augments oxidative stress through the Fenton reaction. Accordingly, hepatic oxidative stress was significantly higher in IP-KO mice than in WT mice after 10 wk of MCDD (Figure 4F), suggesting that augmented oxidative stress in the liver contributes to the progression of steatohepatitis in IP-KO mice. Although the

mechanism leading to hepatic iron overload remains to be clarified, the hepatic expression level of *hepcidin*, a key molecule for iron metabolism, was significantly lower in IP-KO mice than in WT mice (data not shown), indicating a negative feedback response for the greater hepatic iron deposition in IP-KO mice. Since an IP agonist protects cultured hepatocytes from excess iron-induced apoptosis (55), PGI_2 might exert a direct protective action on hepatocytes in steatohepatitis associated with hepatic iron overload.

In conclusion, we have clearly demonstrated that the PGI_2-IP system plays a suppressive role in the development and progression of steatohepatitis. The suppressive role was mediated, at least in part, through the inhibition of Kupffer cell-related inflammatory responses, eventually leading to excess iron accumulation and augmented oxidative stress in the liver. There has been no report indicating the involvement of PGI_2-IP signaling in hepatic protection in NASH patients. However, elevated expression levels of COX-2 mRNA and protein in the liver of NASH patients (8, 56) suggest that increased hepatic production of PGI_2 in NASH patients reinforces PGI_2-IP signaling, resulting in hepatic protection in NASH patients as shown in the present animal NASH model. We propose that stimulation of PGI_2-IP signaling presents a potent therapeutic strategy for NASH.

Acknowledgments

This work was supported by a grant from Core Research for Evolutional Science and Technology (CREST) of Japan Science and Technology Agency (15gm0410006h0106).

This work was also supported by a grant from the Smoking Research Foundation. We thank Y. Watanabe and T. Yokoyama for help in breeding and maintenance of mice. We also thank Y. Tomonari, T. Ohkubo, N. Niizeki and T. Ito for experimental assistance and Y. Takashima for secretarial help. Beraprost was kindly donated from Toray Industries, Inc..

References

1. Torres, D. M., and Harrison, S. A. (2008) Diagnosis and therapy of nonalcoholic steatohepatitis. *Gastroenterology* **134**, 1682-1698
2. Matteoni, C. A., Younossi, Z. M., Gramlich, T., Boparai, N., Liu, Y. C., and McCullough, A. J. (1999) Nonalcoholic fatty liver disease: a spectrum of clinical and pathological severity. *Gastroenterology* **116**, 1413-1419
3. Farrell, G. C., and Larter, C. Z. (2006) Nonalcoholic fatty liver disease: from steatosis to cirrhosis. *Hepatology* **43**, S99-S112
4. Day, C. P., and James, O. F. (1998) Steatohepatitis: a tale of two "hits"? *Gastroenterology* **114**, 842-845
5. Angulo, P. (2002) Nonalcoholic fatty liver disease. *N Engl J Med* **346**, 1221-1231
6. Tilg, H., and Moschen, A. R. (2010) Evolution of inflammation in nonalcoholic fatty liver disease: the multiple parallel hits hypothesis. *Hepatology* **52**, 1836-1846
7. Sanyal, A. J., Chalasani, N., Kowdley, K. V., McCullough, A., Diehl, A. M., Bass, N. M., Neuschwander-Tetri, B. A., Lavine, J. E., Tonascia, J., Unalp, A., Van Natta, M., Clark, J., Brunt, E. M., Kleiner, D. E., Hoofnagle, J. H., Robuck, P. R., and Nash, C. R. N. (2010) Pioglitazone, vitamin E, or placebo for nonalcoholic steatohepatitis. *N Engl J Med* **362**, 1675-1685
8. Giannitrapani, L., Ingrao, S., Soresi, M., Florena, A. M., La Spada, E., Sandonato, L., D'Alessandro, N., Cervello, M., and Montalto, G. (2009) Cyclooxygenase-2 expression in chronic liver diseases and hepatocellular carcinoma: an immunohistochemical study. *Ann N Y Acad Sci* **1155**, 293-299
9. Yu, J., Ip, E., Dela Pena, A., Hou, J. Y., Sesha, J., Pera, N., Hall, P., Kirsch, R., Leclercq, I., and Farrell, G. C. (2006) COX-2 induction in mice with experimental nutritional steatohepatitis: Role as pro-inflammatory mediator. *Hepatology* **43**, 826-836
10. Leclercq, I. A., Farrell, G. C., Sempoux, C., dela Pena, A., and Horsmans, Y. (2004) Curcumin inhibits NF-kappaB activation and reduces the severity of experimental steatohepatitis in mice. *J Hepatol* **41**, 926-934
11. dela Pena, A., Leclercq, I. A., Williams, J., and Farrell, G. C. (2007) NADPH oxidase is not an essential mediator of oxidative stress or liver injury in murine MCD diet-induced steatohepatitis. *J Hepatol* **46**, 304-313

12. Narumiya, S., Sugimoto, Y., and Ushikubi, F. (1999) Prostanoid receptors: structures, properties, and functions. *Physiol Rev* **79**, 1193-1226
13. Bunting, S., Gryglewski, R., Moncada, S., and Vane, J. R. (1976) Arterial walls generate from prostaglandin endoperoxides a substance (prostaglandin X) which relaxes strips of mesenteric and coeliac ateries and inhibits platelet aggregation. *Prostaglandins* **12**, 897-913
14. Moncada, S., Higgs, E. A., and Vane, J. R. (1977) Human arterial and venous tissues generate prostacyclin (prostaglandin x), a potent inhibitor of platelet aggregation. *Lancet* **1**, 18-20
15. Humbert, M., Sitbon, O., and Simonneau, G. (2004) Treatment of pulmonary arterial hypertension. *N Engl J Med* **351**, 1425-1436
16. Xiao, C. Y., Hara, A., Yuhki, K., Fujino, T., Ma, H., Okada, Y., Takahata, O., Yamada, T., Murata, T., Narumiya, S., and Ushikubi, F. (2001) Roles of prostaglandin I(2) and thromboxane A(2) in cardiac ischemia-reperfusion injury: a study using mice lacking their respective receptors. *Circulation* **104**, 2210-2215
17. Hara, A., Yuhki, K., Fujino, T., Yamada, T., Takayama, K., Kuriyama, S., Takahata, O., Karibe, H., Okada, Y., Xiao, C. Y., Ma, H., Narumiya, S., and Ushikubi, F. (2005) Augmented cardiac hypertrophy in response to pressure overload in mice lacking the prostaglandin I2 receptor. *Circulation* **112**, 84-92
18. Fujino, T., Nakagawa, N., Yuhki, K., Hara, A., Yamada, T., Takayama, K., Kuriyama, S., Hosoki, Y., Takahata, O., Taniguchi, T., Fukuzawa, J., Hasebe, N., Kikuchi, K., Narumiya, S., and Ushikubi, F. (2004) Decreased susceptibility to renovascular hypertension in mice lacking the prostaglandin I2 receptor IP. *J Clin Invest* **114**, 805-812
19. Kawada, N., Tran-Thi, T. A., Klein, H., and Decker, K. (1993) The contraction of hepatic stellate (Ito) cells stimulated with vasoactive substances. Possible involvement of endothelin 1 and nitric oxide in the regulation of the sinusoidal tonus. *Eur J Biochem* **213**, 815-823
20. Perez, S., Maldonado, E. N., Aspichueta, P., Ochoa, B., and Chico, Y. (2004) Differential modulation of prostaglandin receptor mRNA abundance by prostaglandins in primary cultured rat hepatocytes. *Mol Cell Biochem* **266**, 183-189
21. Fennekohl, A., Schieferdecker, H. L., Jungermann, K., and Puschel, G. P. (1999) Differential expression of prostanoid receptors in hepatocytes, Kupffer cells, sinusoidal

endothelial cells and stellate cells of rat liver. *J Hepatol* **30**, 38-47

22. Kimura, M., Okamoto, H., Natsume, H., and Ogihara, M. (2009) IP receptor agonist-induced DNA synthesis and proliferation in primary cultures of adult rat hepatocytes: the involvement of endogenous transforming growth factor-alpha. *J Pharmacol Sci* **109**, 618-629
23. Johnston, D. E., and Kroening, C. (1996) Stimulation of prostaglandin synthesis in cultured liver cells by CCl4. *Hepatology* **24**, 677-684
24. Birmelin, M., and Decker, K. (1984) Synthesis of prostanoids and cyclic nucleotides by phagocytosing rat Kupffer cells. *Eur J Biochem* **142**, 219-225
25. Victorov, A. V., and Hoek, J. B. (1995) Secretion of prostaglandins elicited by lipopolysaccharide and ethanol in cultured rat Kupffer cells. *Biochem Biophys Res Commun* **215**, 691-697
26. Eyhorn, S., Schlayer, H. J., Henninger, H. P., Dieter, P., Hermann, R., Woort-Menker, M., Becker, H., Schaefer, H. E., and Decker, K. (1988) Rat hepatic sinusoidal endothelial cells in monolayer culture. Biochemical and ultrastructural characteristics. *J Hepatol* **6**, 23-35
27. Tomasi, V., Meringolo, C., Bartolini, G., and Orlandi, M. (1978) Biosynthesis of prostacyclin in rat liver endothelial cells and its control by prostaglandin E2. *Nature* **273**, 670-671
28. Dorris, S. L., and Peebles, R. S., Jr. (2012) PGI2 as a regulator of inflammatory diseases. *Mediators Inflamm* **2012**, 926968
29. Yin, H., Cheng, L., Langenbach, R., and Ju, C. (2007) Prostaglandin I(2) and E(2) mediate the protective effects of cyclooxygenase-2 in a mouse model of immune-mediated liver injury. *Hepatology* **45**, 159-169
30. Grundmann, H. J., Hahnle, U., Hegenscheid, B., Sahlmuller, G., Bienzle, U., and Blitstein-Willinger, E. (1992) Inhibition of endotoxin-induced macrophage tumor necrosis factor expression by a prostacyclin analogue and its beneficial effect in experimental lipopolysaccharide intoxication. *J Infect Dis* **165**, 501-505
31. Corbin, K. D., and Zeisel, S. H. (2012) Choline metabolism provides novel insights into nonalcoholic fatty liver disease and its progression. *Curr Opin Gastroenterol* **28**, 159-165
32. Mato, J. M., Corrales, F. J., Lu, S. C., and Avila, M. A. (2002) S-Adenosylmethionine: a control switch that regulates liver function. *FASEB J* **16**, 15-26

33. Murata, T., Ushikubi, F., Matsuoka, T., Hirata, M., Yamasaki, A., Sugimoto, Y., Ichikawa, A., Aze, Y., Tanaka, T., Yoshida, N., Ueno, A., Oh-ishi, S., and Narumiya, S. (1997) Altered pain perception and inflammatory response in mice lacking prostacyclin receptor. *Nature* **388**, 678-682

34. Akiba, T., Miyazaki, M., and Toda, N. (1986) Vasodilator actions of TRK-100, a new prostaglandin I2 analogue. *Br J Pharmacol* **89**, 703-711

35. Kleiner, D. E., Brunt, E. M., Van Natta, M., Behling, C., Contos, M. J., Cummings, O. W., Ferrell, L. D., Liu, Y. C., Torbenson, M. S., Unalp-Arida, A., Yeh, M., McCullough, A. J., Sanyal, A. J., and Nonalcoholic Steatohepatitis Clinical Research, N. (2005) Design and validation of a histological scoring system for nonalcoholic fatty liver disease. *Hepatology* **41**, 1313-1321

36. Lee, S. H., Starkey, P. M., and Gordon, S. (1985) Quantitative analysis of total macrophage content in adult mouse tissues. Immunochemical studies with monoclonal antibody F4/80. *J Exp Med* **161**, 475-489

37. Requena, J. R., Fu, M. X., Ahmed, M. U., Jenkins, A. J., Lyons, T. J., and Thorpe, S. R. (1996) Lipoxidation products as biomarkers of oxidative damage to proteins during lipid peroxidation reactions. *Nephrol Dial Transplant* **11 Suppl 5**, 48-53

38. Walker, R. J., Miller, J. P., Dymock, I. W., Shilkin, K. B., and Williams, R. (1971) Relationship of hepatic iron concentration to histochemical grading and to total chelatable body iron in conditions associated with iron overload. *Gut* **12**, 1011-1014

39. Nakagawa, N., Yuhki, K., Kawabe, J., Fujino, T., Takahata, O., Kabara, M., Abe, K., Kojima, F., Kashiwagi, H., Hasebe, N., Kikuchi, K., Sugimoto, Y., Narumiya, S., and Ushikubi, F. (2012) The intrinsic prostaglandin E2-EP4 system of the renal tubular epithelium limits the development of tubulointerstitial fibrosis in mice. *Kidney Int* **82**, 158-171

40. Rizki, G., Arnaboldi, L., Gabrielli, B., Yan, J., Lee, G. S., Ng, R. K., Turner, S. M., Badger, T. M., Pitas, R. E., and Maher, J. J. (2006) Mice fed a lipogenic methionine-choline-deficient diet develop hypermetabolism coincident with hepatic suppression of SCD-1. *J Lipid Res* **47**, 2280-2290

41. Tosello-Trampont, A. C., Landes, S. G., Nguyen, V., Novobrantseva, T. I., and Hahn, Y. S. (2012) Kuppfer cells trigger nonalcoholic steatohepatitis development in diet-induced mouse model through tumor necrosis factor-alpha production. *J Biol Chem* **287**, 40161-40172

42. Tomita, K., Tamiya, G., Ando, S., Ohsumi, K., Chiyo, T., Mizutani, A., Kitamura, N., Toda, K., Kaneko, T., Horie, Y., Han, J. Y., Kato, S., Shimoda, M., Oike, Y., Tomizawa, M., Makino, S., Ohkura, T., Saito, H., Kumagai, N., Nagata, H., Ishii, H., and Hibi, T. (2006) Tumour necrosis factor alpha signalling through activation of Kupffer cells plays an essential role in liver fibrosis of non-alcoholic steatohepatitis in mice. *Gut* **55**, 415-424

43. Velayudham, A., Dolganiuc, A., Ellis, M., Petrasek, J., Kodys, K., Mandrekar, P., and Szabo, G. (2009) VSL#3 probiotic treatment attenuates fibrosis without changes in steatohepatitis in a diet-induced nonalcoholic steatohepatitis model in mice. *Hepatology* **49**, 989-997

44. Marra, F., and Tacke, F. (2014) Roles for chemokines in liver disease. *Gastroenterology* **147**, 577-594 e571

45. Haukeland, J. W., Damas, J. K., Konopski, Z., Loberg, E. M., Haaland, T., Goverud, I., Torjesen, P. A., Birkeland, K., Bjoro, K., and Aukrust, P. (2006) Systemic inflammation in nonalcoholic fatty liver disease is characterized by elevated levels of CCL2. *J Hepatol* **44**, 1167-1174

46. Miura, K., Yang, L., van Rooijen, N., Ohnishi, H., and Seki, E. (2012) Hepatic recruitment of macrophages promotes nonalcoholic steatohepatitis through CCR2. *Am J Physiol Gastrointest Liver Physiol* **302**, G1310-1321

47. Henao-Mejia, J., Elinav, E., Jin, C., Hao, L., Mehal, W. Z., Strowig, T., Thaiss, C. A., Kau, A. L., Eisenbarth, S. C., Jurczak, M. J., Camporez, J. P., Shulman, G. I., Gordon, J. I., Hoffman, H. M., and Flavell, R. A. (2012) Inflammasome-mediated dysbiosis regulates progression of NAFLD and obesity. *Nature* **482**, 179-185

48. Yeh, C. H., Kuo, C. H., Yang, S. N., Huang, M. Y., Wu, H. C., Wang, H. P., Kuo, T. H., and Hung, C. H. (2011) Prostaglandin I2 analogs suppress tumor necrosis factor alpha production and the maturation of human monocyte-derived dendritic cells. *J Investig Med* **59**, 1109-1115

49. Koek, G. H., Liedorp, P. R., and Bast, A. (2011) The role of oxidative stress in non-alcoholic steatohepatitis. *Clin Chim Acta* **412**, 1297-1305

50. Pietrangelo, A. (2009) Iron in NASH, chronic liver diseases and HCC: how much iron is too much? *J Hepatol* **50**, 249-251

51. Valenti, L., Fracanzani, A. L., Bugianesi, E., Dongiovanni, P., Galmozzi, E., Vanni, E., Canavesi, E., Lattuada, E., Roviaro, G., Marchesini, G., and Fargion, S. (2010) HFE genotype, parenchymal iron accumulation, and liver fibrosis in patients with

nonalcoholic fatty liver disease. *Gastroenterology* **138**, 905-912

52. Nelson, J., Gibbons, E., Pickett, K. R., Streeter, M., Warcup, A. O., Yeung, C. H., Judd, A. M., and Bell, J. D. (2011) Relationship between membrane permeability and specificity of human secretory phospholipase A(2) isoforms during cell death. *Biochim Biophys Acta* **1808**, 1913-1920

53. Sumida, Y., Kanemasa, K., Fukumoto, K., Yoshida, N., Sakai, K., Nakashima, T., and Okanoue, T. (2006) Effect of iron reduction by phlebotomy in Japanese patients with nonalcoholic steatohepatitis: A pilot study. *Hepatol Res* **36**, 315-321

54. Yoneda, M., Nozaki, Y., Endo, H., Mawatari, H., Iida, H., Fujita, K., Yoneda, K., Takahashi, H., Kirikoshi, H., Inamori, M., Kobayashi, N., Kubota, K., Saito, S., Maeyama, S., Hotta, K., and Nakajima, A. (2010) Serum ferritin is a clinical biomarker in Japanese patients with nonalcoholic steatohepatitis (NASH) independent of HFE gene mutation. *Dig Dis Sci* **55**, 808-814

55. Lee, F. P., Jen, C. Y., Chang, C. C., Chou, Y., Lin, H., Chou, C. M., and Juan, S. H. (2010) Mechanisms of adiponectin-mediated COX-2 induction and protection against iron injury in mouse hepatocytes. *J Cell Physiol* **224**, 837-847

56. Lima-Cabello, E., Garcia-Mediavilla, M. V., Miquilena-Colina, M. E., Vargas-Castrillon, J., Lozano-Rodriguez, T., Fernandez-Bermejo, M., Olcoz, J. L., Gonzalez-Gallego, J., Garcia-Monzon, C., and Sanchez-Campos, S. (2011) Enhanced expression of pro-inflammatory mediators and liver X-receptor-regulated lipogenic genes in non-alcoholic fatty liver disease and hepatitis C. *Clin Sci (Lond)* **120**, 239-250

Figure legends

Figure 1. PGI_2-IP signaling is reinforced during MCDD feeding. Expression levels of *Cox-1* and *Cox-2* mRNAs (**A**), *Pgis* mRNA (**B**) and *Ip* mRNA (**C**) in the liver of WT mice during MCDD feeding. The amounts of amplification products of the respective mRNAs were normalized to that of *18s* rRNA, and the value at 0 wk of MCDD is presented as 1. $n = 6$-11. $^{*}P < .05$ vs. 0 wk.

Figure 2. MCDD-induced steatohepatitis develops earlier in IP-KO mice than in WT mice. (**A**) Representative HE-stained sections of the liver prepared from WT and IP-KO mice fed MCDD for 0, 5 and 10 wk. Scale bars: 100 μm. (**B** and **C**) Histological alterations of the liver during MCDD feeding were evaluated by use of NAFLD activity score. $n = 7$-14. $^{*}P < .05$ vs. corresponding WT mice.

Figure 3. Facilitated development of steatohepatitis in IP-KO mice is accompanied by augmented histological derangements and hepatocyte damage. (**A**) Representative Oil Red O-stained cryosections of the liver prepared from WT and IP-KO mice at 5 wk of ND or MCDD. Scale bars: 100 μm. (**B**) Quantification of TG in the livers of WT and IP-KO mice at 5 wk of ND or MCDD feeding. $n = 6$-14. $^{*}P < .05$ vs. corresponding WT mice. (**C**) Representative sections showing F4/80-positive cells (brown color) in the livers prepared from WT and IP-KO mice at 5 wk of ND or MCDD. Scale bars: 50 μm. (**D**)

Inflammatory cell accumulation in the livers of WT and IP-KO mice at 5 wk of ND or MCDD was evaluated by counting the numbers of F4/80-positive cells. $n = 4$-13. $^{*}P < .05$ vs. corresponding WT mice. **(E)** Serum transaminase levels of WT and IP-KO mice at 5 wk of MCDD. WT: $n = 13$. IP-KO: $n = 15$. $^{*}P < .05$ vs. corresponding WT mice.

Figure 4. Augmented oxidative stress and increased MCP-1 and TNF-α contents in the livers of IP-KO mice after MCDD feeding. **(A)** Hepatic iron contents of WT and IP-KO mice were measured by atomic absorption spectrophotometry at 0, 2, 5 and 10 wk of MCDD. $n = 7$-15. $^{*}P < .05$ vs. 0 wk. $^{**}P < .05$ vs. corresponding WT mice. **(B)** Serum ferritin levels at 0, 2, 5 and 10 wk of MCDD. $n = 6$-15. $^{*}P < .05$ vs. 0 wk. $^{**}P < .05$ vs. corresponding WT mice. **(C)** Representative Berlin blue-stained sections of the livers prepared from WT and IP-KO mice fed ND or MCDD for 10 wk. The lower panels show enlarged photomicrographs of the areas indicated by the boxes in the corresponding middle panels. Scale bars: 200 μm (upper and middle panels) and 50 μm (lower panels). **(D)** Representative liver sections double-stained by Berlin blue and the anti-F4/80 antibody system in IP-KO mice fed MCDD for 10 wk. Iron accumulation was detected mainly in hepatocytes (arrows in the right panel) and in a few F4/80-positive cells (arrows in the left panel). Scale bars: 25 μm. **(E)** Representative sections stained by the anti-4-HNE antibody system (brown color) of the livers prepared from WT and IP-KO mice fed ND or MCDD for 10 wk. Scale bars: 100 μm. **(F)** Hepatic contents of TBARS, a marker of lipid peroxidation, were measured in WT and IP-KO mice at 0, 2, 5 and 10 wk of MCDD.

n = 6-10. $^{*}P < .05$ vs. corresponding WT mice. (**G** and **H**) Hepatic contents of MCP-1 (**G**) and TNF-α (**H**) in WT and IP-KO mice at 0, 2, 5 and 10 wk of MCDD. MCP-1: n = 6-19. TNF-α: n = 6-15. $^{*}P < .05$ vs. 0 wk. $^{**}P < .05$ vs. corresponding WT mice.

Figure 5. Beraprost suppresses the development of steatohepatitis in WT mice fed MCDD. (**A**) Representative HE-stained sections of the livers prepared from beraprost-treated and untreated WT and IP-KO mice fed MCDD for 10 wk. Scale bars: 100 μm. (**B** and **C**) Effects of beraprost on NAFLD activity score in WT mice at 2, 5 and 10 wk of MCDD and in IP-KO mice at 10 wk of MCDD. WT mice: n = 6-13. Control IP-KO mice: n = 12. Beraprost-treated IP-KO mice: n = 5. $^{*}P < .05$ vs. corresponding control. (**D**) Representative sections stained by the anti-F4/80 antibody system of the livers prepared from beraprost-treated and untreated WT mice fed MCDD for 10 wk. Scale bars: 100 μm (upper panels) and 50 μm (lower panels). (**E**) Effect of beraprost on F4/80-positive cell accumulation in the liver of WT mice at 10 wk of MCDD. Control: n = 6. Beraprost: n = 9. $^{*}P < .05$ vs. control. (**F**) Effects of beraprost on serum transaminase levels in WT mice at 2, 5 and 10 wk of MCDD and in IP-KO mice at 10 wk of MCDD. WT mice: n = 6-14. Control IP-KO mice: n = 13. Beraprost-treated IP-KO mice: n = 7. $^{*}P < .05$ vs. corresponding control. (**G** and **H**) Effects of beraprost on hepatic contents of MCP-1 (**G**) and TNF-α (**H**) in WT mice at 2, 5 and 10 wk of MCDD. MCP-1: n = 5-12. TNF-α: n = 5-11. $^{*}P < .05$ vs. corresponding control. BPS: Beraprost.

Figure 6. Beraprost suppresses the LPS-induced expression of mRNAs for *Mcp-1* and *Tnf-α* in cultured Kupffer cells that express *Ip* and produce PGI_2. **(A)** *Ip* mRNA expression in primary cultured Kupffer cells prepared from WT mice. **(B)** PGI_2 production by primary cultured hepatocytes and Kupffer cells prepared from WT mice. n = 6-12. $^{*}P < .05$ vs. control. **(C-F)** Suppressive effects of beraprost on LPS-induced *Mcp-1* **(C and D)** and *Tnf-α* **(E and F)** mRNA expressions in cultured Kupffer cells prepared from WT **(C and E)** and IP-KO **(D and F)** mice. n = 3-7. $^{*}P < .05$ vs. control. LPS: lipopolysaccharide. BPS: Beraprost.

Table 1. Changes in nutritional and metabolic conditions induced by MCDD feeding

Time on diet	0 wk		5 wk		10 wk			
Genotype	WT	IP-KO	WT MCD	IP-KO MCD	WT ND	WT MCD	IP-KO ND	IP-KO MCD
BW (g)	22.0 ± 0.4	24.6 ± 0.7*	16.0 ± 0.5	17.2 ± 0.5	29.6 ± 1.0	14.7 ± 0.2	30.7 ± 0.7	14.4 ± 0.6
LW (g)	1.31 ± 0.04	1.37 ± 0.12	0.56 ± 0.02	0.65 ± 0.03	1.57 ± 0.07	0.55 ± 0.03	1.52 ± 0.05	0.57 ± 0.04
eWAT-W (mg)	250 ± 21	228 ± 24	86 ± 13	70 ± 11	631 ± 100	66 ± 12	408 ± 51	30 ± 20
BS (g/dL)	173 ± 9	160 ± 9	97 ± 5	97 ± 4	147 ± 3	84 ± 5	152 ± 5	76 ± 6
TG (g/dL)	50 ± 11	40 ± 7	20 ± 2	19 ± 3	98 ± 8	14 ± 1	65 ± 12	16 ± 4
T-chol (g/dL)	95 ±10	74 ± 10	40 ± 3	29 ± 2	86 ± 5	25 ± 3	80 ± 5	34 ± 10

BW, body weight; LW, liver weight; eWAT-W, epididymal white adipose tissue weight; BS, blood sugar; TG, triglyceride; T-chol, total cholesterol. BW, LW, eWAT-W and BS: WT mice (n = 6-15), IP-KO mice (n = 7-17), respectively. TG and T-chol: WT mice (n = 3-13), IP-KO mice (n = 4-15), respectively. *$P < .05$ vs. corresponding WT mice.

Figure 1

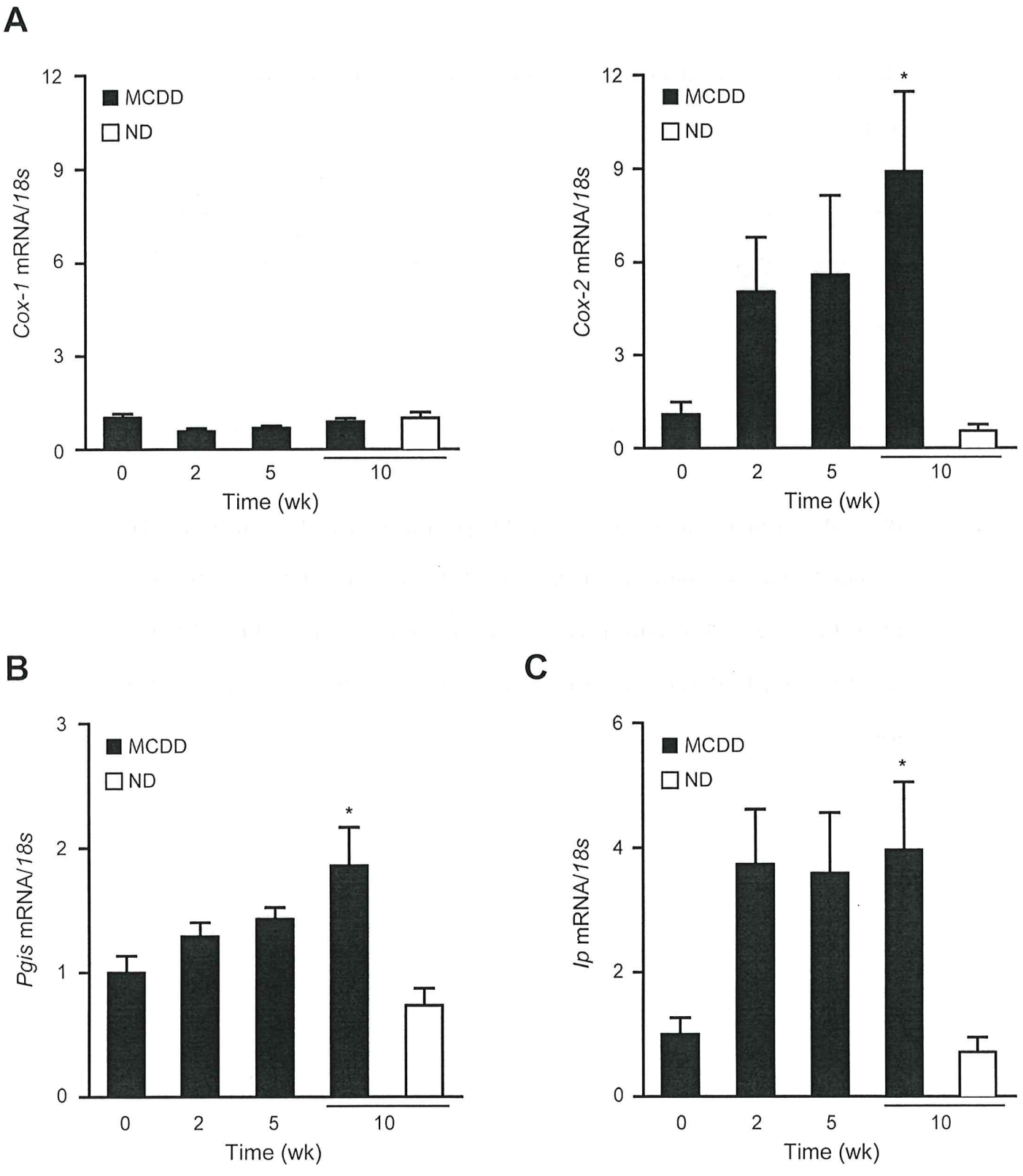
A
Cox-1 mRNA/18s
MCDD
ND
12
9
6
3
0
0
2
5
10
Time (wk)
Cox-2 mRNA/18s
*
B
Pgis mRNA/18s
C
Ip mRNA/18s

Figure 2

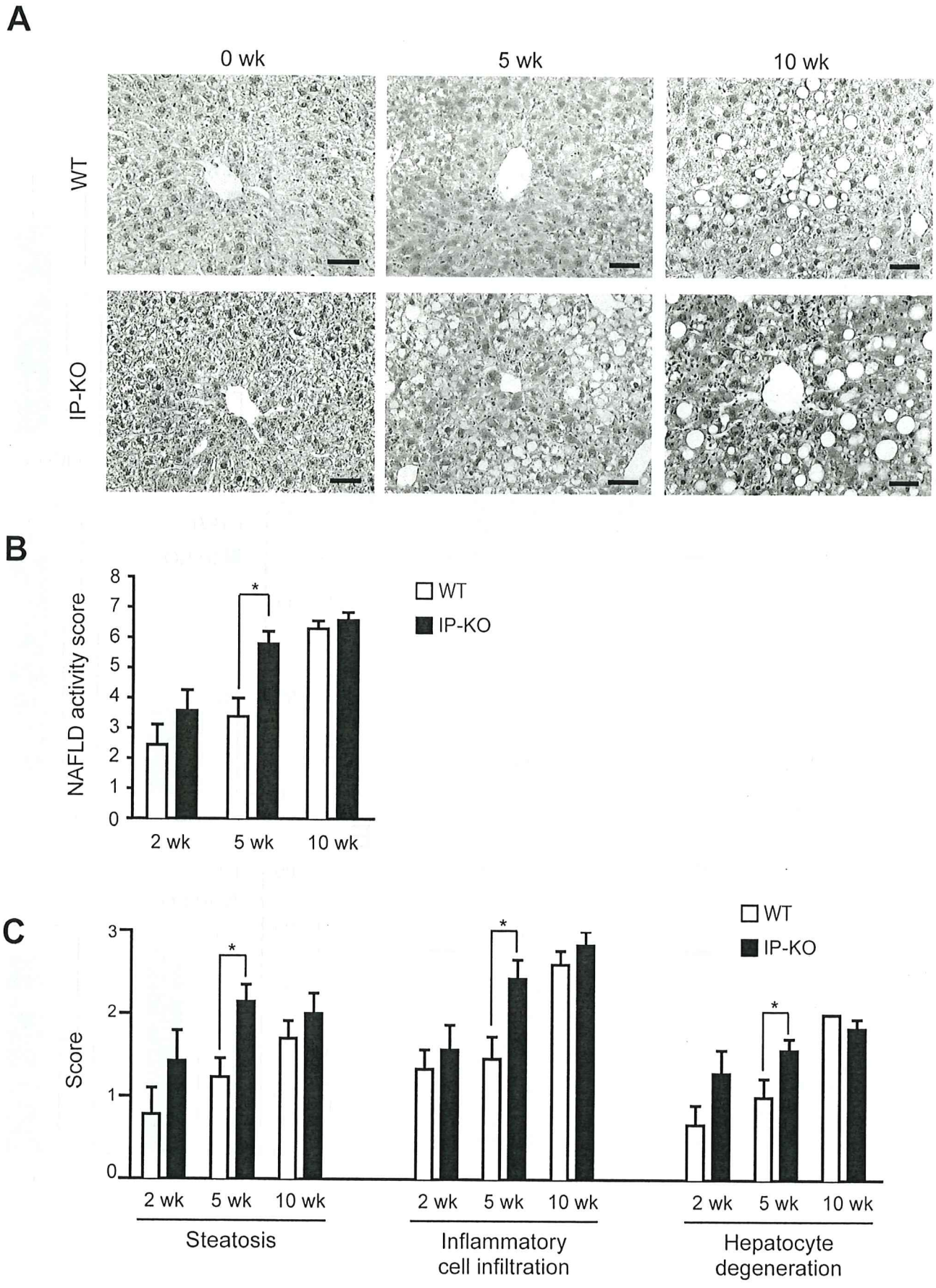
A
0 wk
5 wk
10 wk
WT
IP-KO
B
NAFLD activity score
0
1
2
3
4
5
6
7
8
*
WT
IP-KO
2 wk
5 wk
10 wk
C
Score
0
1
2
3
*
*
*
WT
IP-KO
2 wk
5 wk
10 wk
Steatosis
Inflammatory cell infiltration
Hepatocyte degeneration

Figure 3

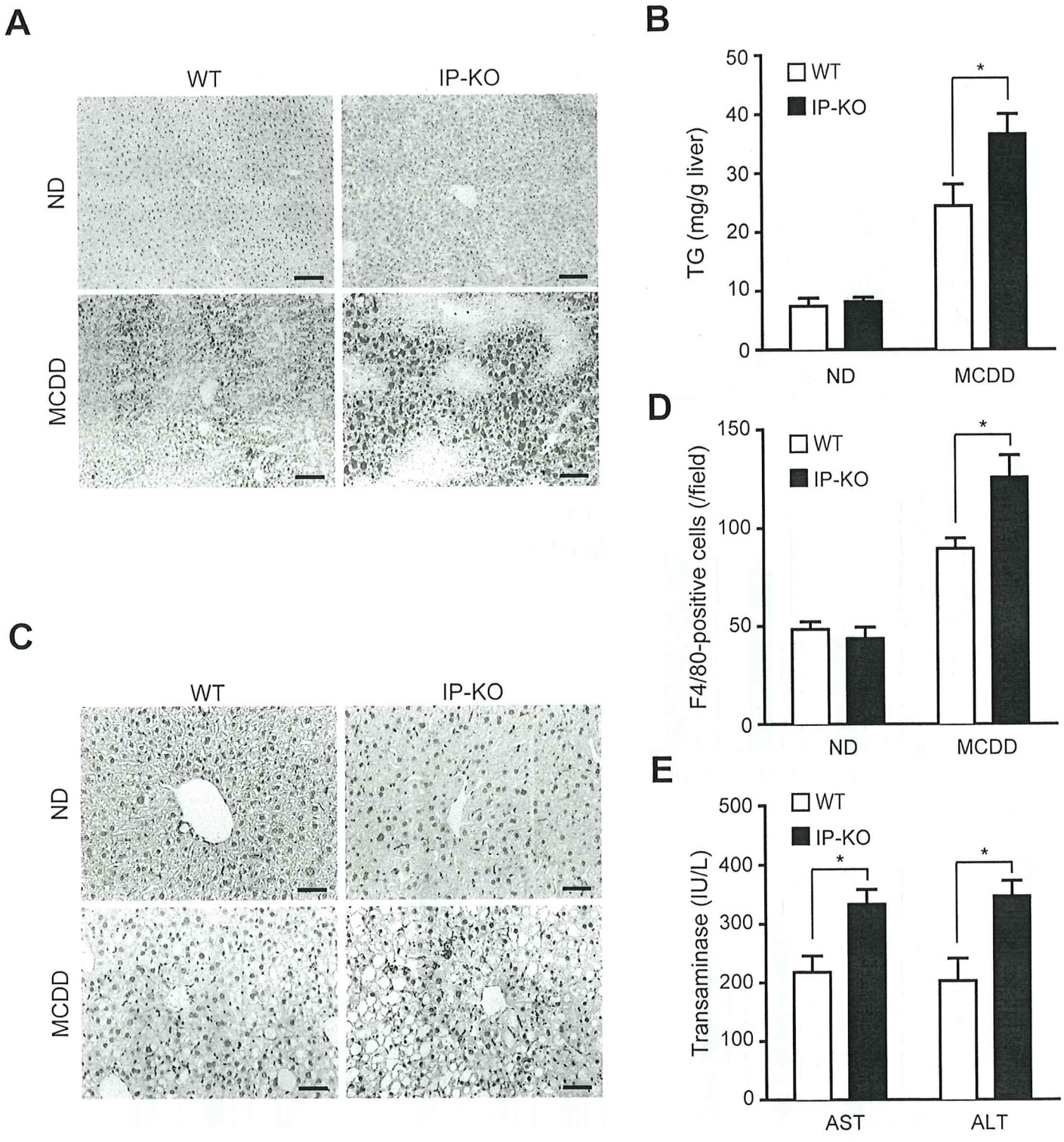
A
WT
IP-KO
ND
MCDD
B
WT
IP-KO
TG (mg/g liver)
50
40
30
20
10
0
*
ND
MCDD
C
WT
IP-KO
ND
MCDD
D
WT
IP-KO
F4/80-positive cells (/field)
150
100
50
0
*
ND
MCDD
E
WT
IP-KO
Transaminase (IU/L)
500
400
300
200
100
0
*
*
AST
ALT

Figure 4

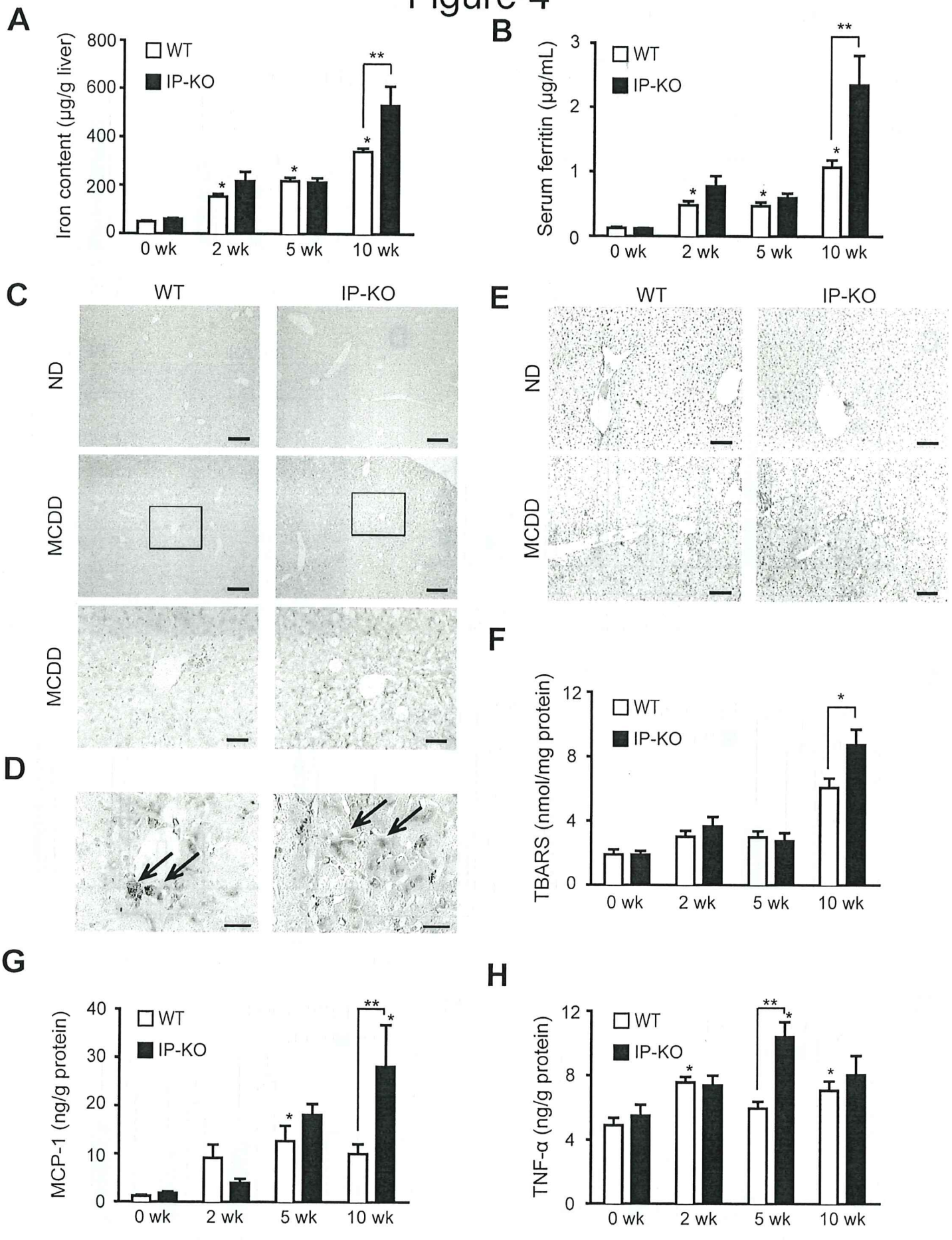
A
Iron content (μg/g liver)
800
600
400
200
0
WT
IP-KO
0 wk
2 wk
5 wk
10 wk
B
Serum ferritin (μg/mL)
3
2
1
0
C
WT
IP-KO
ND
MCDD
MCDD
D
E
F
TBARS (nmol/mg protein)
12
8
4
G
MCP-1 (ng/g protein)
40
30
20
10
H
TNF-α (ng/g protein)

Figure 5B

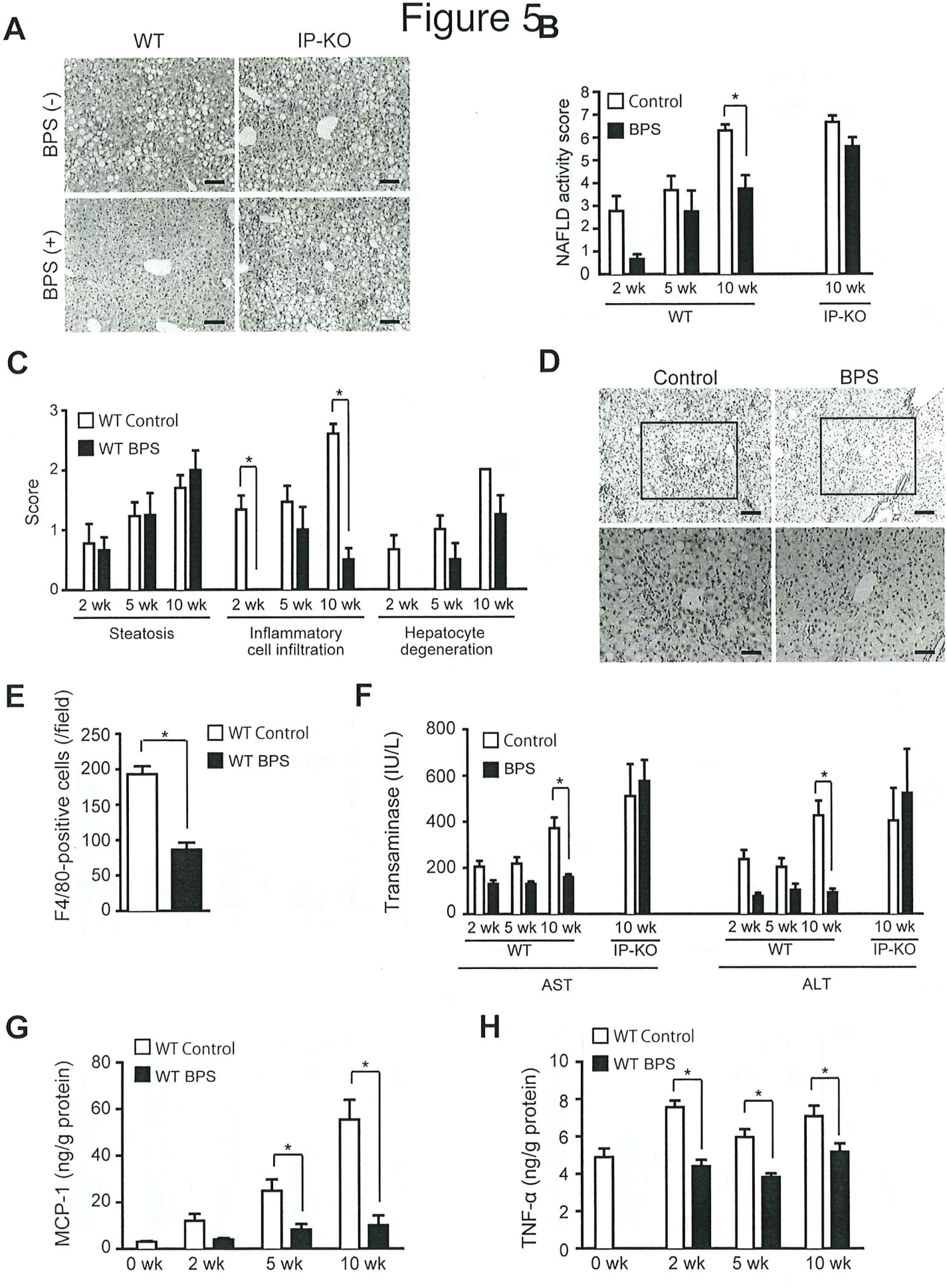
A
WT
IP-KO
BPS (-)
BPS (+)
NAFLD activity score
Control
BPS
2 wk
5 wk
10 wk
WT
IP-KO
C
Score
WT Control
WT BPS
Steatosis
Inflammatory cell infiltration
Hepatocyte degeneration
D
Control
BPS
E
F4/80-positive cells (/field)
F
Transaminase (IU/L)
AST
ALT
G
MCP-1 (ng/g protein)
0 wk
H
TNF-α (ng/g protein)

Figure 6

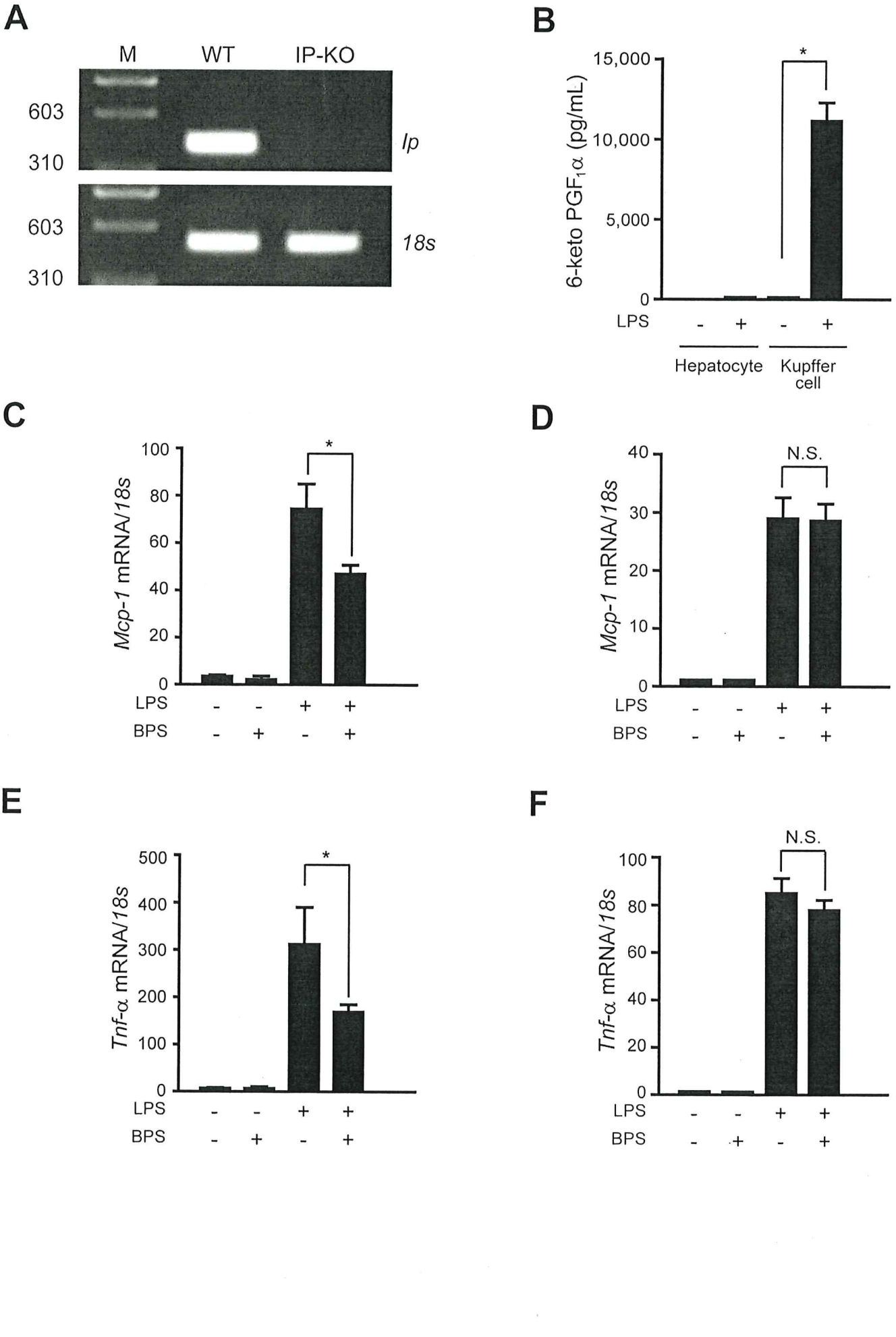
A
M
WT
IP-KO
603
310
Ip
603
310
18s
B
6-keto PGF1α (pg/mL)
15,000
10,000
5,000
0
*
LPS
- + - +
Hepatocyte
Kupffer cell
C
Mcp-1 mRNA/18s
100
80
60
40
20
0
*
LPS - - + +
BPS - + - +
D
Mcp-1 mRNA/18s
40
30
20
10
0
N.S.
LPS - - + +
BPS - + - +
E
Tnf-α mRNA/18s
500
400
300
200
100
0
*
LPS - - + +
BPS - + - +
F
Tnf-α mRNA/18s
100
80
60
40
20
0
N.S.
LPS - - + +
BPS - + - +